Vibrationally quantum-state-specific dynamics of the reactions of CN radicals with organic molecules in solution

Rebecca A. Rose,[1] Stuart J. Greaves,[1] Thomas A.A. Oliver,[1] Ian P. Clark,[2] Gregory M. Greetham,[2] Anthony W. Parker,[2] Michael Towrie[2] and Andrew J. Orr-Ewing[1,*]

[1] *School of Chemistry, University of Bristol, Cantock's Close, Bristol BS8 1TS, UK*

[2] *Central Laser Facility, Research Complex at Harwell, Science and Technology Facilities Council, Rutherford Appleton Laboratory, Harwell Science and Innovation Campus, Didcot, Oxfordshire, OX11 0QX, UK*

20 April 2011

* Author for correspondence

Tel: +44 117 9287672

Fax: +44 117 9250612

e-mail: a.orr-ewing@bris.ac.uk

Abstract

The dynamics of reactions of CN radicals with cyclohexane, d_{12}-cyclohexane, and tetramethylsilane have been studied in solutions of chloroform, dichloromethane and the deuterated variants of these solvents using ultraviolet photolysis of ICN to initate reaction. The H(D)-atom abstraction reactions produce HCN (DCN) that is probed in absorption with sub-picosecond time resolution using ~500 cm^{-1} bandwidth infrared (IR) pulses in the spectral regions corresponding to C–H (or C–D) and C≡N stretching mode fundamental and hot bands. Equivalent IR spectra were obtained for the reactions of CN radicals with the pure solvents. In all cases, the reaction products are formed at early times with a strong propensity for vibrational excitation of the C–H (or C–D) stretching (v_3) and H–C–N (D–C–N) bending (v_2) modes, and for DCN products there is also evidence of vibrational excitation of the v_1 mode, which involves stretching of the C≡N bond. The vibrationally excited products relax to the ground vibrational level of HCN (DCN) with time constants of ~130 – 270 ps (depending on molecule and solvent), and the majority of the HCN (DCN) in this ground level is formed by vibrational relaxation, instead of directly from the chemical reaction. The time-dependence of reactive production of HCN (DCN) and vibrational relaxation is analysed using a vibrationally quantum-state specific kinetic model. The experimental outcomes are indicative of dynamics of exothermic reactions over an energy surface with an early transition state. Although the presence of the chlorinated solvent may reduce the extent of vibrational excitation of the nascent products, the early-time chemical reaction dynamics in these liquid solvents are deduced to be very similar to those for isolated collisions in the gas phase. The transient IR spectra show additional spectroscopic absorption features centered at 2037 cm^{-1} and 2065 cm^{-1} (in $CHCl_3$) that are assigned, respectively, to CN-solvent complexes and recombination of I atoms with CN radicals to form INC molecules. These products build up rapidly, with respective time constants of 8–26 and 11–22 ps. A further, slower rise in the INC absorption signal (with time constant >500 ps) is attributed to diffusive recombination after escape from the initial solvent cage and accounts for more than 2/3 of the observed INC.

1. Introduction

Current understanding of the fundamental mechanisms of chemical reactions has developed from a combination of experimental measurements that probe nascent reaction products and theoretical calculations of potential energy surfaces (PESs) and scattering dynamics.[1,2] For gas-phase and gas-surface reactions, for which isolated collisions can be examined, experimental methods are well established that can resolve disposal of energy into product translational, rotational, vibrational and electronic degrees of freedom, together with preferred directions of scatter.[1,2,3] In an increasing number of cases, direct comparisons can be made with computational predictions to probe ever more deeply the features of the PESs which govern how these reactions evolve.

Many reactions of biological and chemical importance occur in solution under conditions of frequent collisions with the surrounding solvent molecules, yet much less is known about how the reaction dynamics change as a result of solvent interactions.[4,5,6] Detection of nascent reaction products in solution requires measurements to be made on an ultrafast (femto- or pico-second) timescale, before collisions with the solvent molecules relax any quantum-state specific signatures of product excitation. Spectral features are broadened by interactions with the solvent, and information available from gas-phase experiments, for isolated molecules that can undergo free rotational and translational motion, is lost. Thus, several previous studies of reactions in solution have focussed on rates of appearance of ground-state reaction products and the formation of complexes.[7,8,9,10,11,12,13] Nonetheless, experiments by Hochstrasser and co-workers demonstrated the possibility of observing vibrationally excited reaction products in solution;[8] 19±6% of DCN from the reaction of CN radicals with deuterated liquid chloroform was shown to be formed with one quantum of C–D stretch excitation. In a recent publication, we demonstrated significantly greater C–H stretch and bending vibrational mode excitation of HCN products of the exothermic reaction of CN radicals with cyclohexane in solution in chlorinated organic solvents.[14] The experiment employed ultraviolet (UV) pump and broadband infrared (IR) absorption spectroscopy probe methods with sub-picosecond time resolution, and showed that chemical dynamics in

solution in bulk liquids could be investigated at a level of detail approaching that for gas-phase and gas-surface reactions.

Here, we report more extensive observations of the dynamics of the H-atom abstraction reactions of CN radicals with small organic molecules (RH), CN + RH → HCN + R, in solution in common chlorinated solvents, and the analogous reaction with deuterated organic molecules (RD). Such reactions are typically exothermic by ~10 000 cm^{-1}, which is sufficient energy for population of up to 3 quanta of C–H stretch (the v_3 mode; up to 4 quanta of the equivalent C–D stretch in DCN), 4 quanta of C≡N stretch (the v_1 mode) or ~14 quanta of bending vibration (the v_2 mode). We use the nascent populations of the vibrational modes of HCN as a probe for the dynamics of the reaction. The IR spectroscopy of HCN and DCN in the gas phase is well known and the anharmonicities of the vibrational modes enable the spectral signatures of vibrationally excited products to be resolved.[15,16]

In order to unravel the influence of the solvent on the reaction it is useful to compare our studies in solution with those of the well-characterized solvent-free dynamics of CN + RH reactions in the gas phase.[17,18,19,20,21,22] These studies show that HCN is formed with substantial vibrational excitation in both the C–H stretch and bending modes. For the reactions of CN radicals with a range of small organic molecules (methane, ethane, propane, cyclopropane, isobutane, neopentane and chloroform), Jackson and co-workers reported that up to 2 quanta of C–H stretch are excited and a population inversion is observed between the v_3=2 and v_3=1 vibrational levels for all except the reactions with methane and cyclopropane.[19,22] Complementary experiments led Macdonald and coworkers to conclude that almost every (>99%) HCN product of the reaction of CN with ethane is formed with the bending vibrational mode excited above its zero-point level.[18] However, excited levels of the C≡N stretching mode were not observed to be significantly populated.[18,23]

The work presented here extends our investigations of the reactions of CN with cyclohexane in solution in dichloromethane (CH_2Cl_2), chloroform ($CHCl_3$) or deuterated chloroform ($CDCl_3$)[14] to include solute concentration dependent data, and examines the dynamics of reactions of CN radicals with tetramethylsilane (TMS) in

CH_2Cl_2 and $CDCl_3$. The dynamics of H atom abstraction from primary and secondary sites are thus compared, as are H and D atom abstractions to form HCN and DCN. In addition, we report results of the reactions of CN radicals with the pure solvents CH_2Cl_2 and $CHCl_3$. In all cases, broadband transient IR absorption spectroscopy with ps time resolution probes the vibrational excitation of the nascent HCN (DCN) products formed in both the C–H (or C–D) and C≡N stretching regions of the IR spectrum, and the subsequent vibrational relaxation by the solvent bath. An extensive body of data is therefore presented for the dynamics of liquid phase reactions of CN radicals.

2. Experimental

Experiments were conducted using the ULTRA laser system at the Central Laser Facility at the Rutherford Appleton Laboratory. The capabilities of the ULTRA instrument are described in detail elsewhere, [14,24] therefore only details pertinent to the current study are reported here. A 65 MHz titanium:sapphire oscillator seeded a regenerative amplifier operating at 10 kHz repetition rate and configured to produce 40-80 fs duration pulses at wavelength of 800 nm. Third harmonic generation of the 800 nm output of the amplifier produced ~50 fs duration UV pump pulses at 266-nm for ICN photodissociation to generate CN radicals. Approximately 0.4 mJ of the fs, broadband output pulse train of the amplifier pumped an optical parametric amplifier (OPA), and difference frequency mixing of the signal and the idler components generated mid-IR probe pulses with ~500 cm^{-1} bandwidth and ~50 fs pulse duration at the output of the OPA. The UV pulses were polarized at magic angle to the IR probe laser polarization.

Solutions of ICN (98%; Acros Organics) and cyclohexane (>99.9%; Sigma Aldrich), d_{12}-cyclohexane (99.6 atom%; Sigma Aldrich) or TMS (>99.9%; Sigma Aldrich) in chlorinated solvents $CHCl_3$ (>99.8%, Sigma Aldrich), CH_2Cl_2 (>99.6%; Sigma Aldrich) or $CDCl_3$ (99.96 atom%; Sigma Aldrich) were continuously flowed through a Harrick cell with a 0.38-mm thick PTFE spacer between BaF_2 or CaF_2 windows. Reaction was initiated by intersection of the UV pulses with the flowing sample to generate CN radicals by photodissociation of ICN, a process which is known to

produce CN radicals which are ~98% are in their ground vibrational level with high rotational excitation.[25,26] Transient IR absorption spectra were obtained using the mid-IR pulses, focused to ~75 μm spotsize, with a centre frequency selected to probe the C–H stretching region (~3260 cm^{-1}) of HCN, the C≡N stretching region (~2095 cm^{-1} in HCN, ~1920 cm^{-1} in DCN) or the C–D stretching region (~2600 cm^{-1}) of DCN. The IR radiation transmitted by the solution was dispersed by a grating onto a pair of 128-element mercury-cadmium telluride array detectors (IR Associates), providing full (i.e. ~500 cm^{-1}) spectral coverage with every laser pulse. The overall instrument response time was ~200 fs. A reference spectrum of the laser pulse (before the Harrick cell) was accumulated on a third, 64-element array detector and used to remove the effects of laser fluctuations from transient absorption data. Shot-to-shot subtraction methods removed solvent absorption bands and identified transient features resulting from the UV-initiated chemistry. In all experiments, the initial ICN concentration was 0.14 M, and the concentration of the cyclohexane or TMS was 0.0, 0.75, 1.0 or 1.5 M. Spectra were obtained at selected, but randomly ordered, time delays between the UV and IR pulses in the range 1 – 1300 ps which were controlled using a motorised delay stage on the UV beam path. The IR absorption bands of the solvent did not overlap significantly the HCN bands studied, but in the case of DCN spectra, there are some interferences from weak solvent bands. The low extinction coefficient of ICN necessitated use of ≤ 2 μJ energies per UV pulse in an ~150 μm spotsize to generate CN radicals. This resulted in the HCN transient signal being offset by a broad background signal caused by sample heating by the pump laser, and the data presented here have had this offset subtracted.

In some solutions, the CN radicals may react not only with the cyclohexane or TMS solute, but also with the solvent to produce the probed product. The contribution of reaction with solvent to the signals was determined by measuring the time-dependent IR spectra of solutions comprised only of ICN and solvent following UV laser excitation under otherwise identical conditions, just prior to or after the measurements for solutions also containing the cyclohexane or TMS. Integrated band intensities for the former spectra were then subtracted from those for the latter spectra obtained at identical pump-probe time delays to remove the contribution of the reaction with the

solvent. Additionally, analysis of the ICN/solvent sample spectra allowed the investigation of the dynamics of the reaction of CN radicals with the pure solvent.

In a small subset of experiments, transient IR spectra were recorded over nano- to micro-second time scales after initiation of the reaction. In these experiments, the 266 nm photolysis laser wavelength required to photolyse ICN was generated from the fourth harmonic output of a 10 kHz Nd:YVO_4 laser with nanosecond pulse duration and output power of 40 mW. Transient spectra were recorded using the same broadband ultrafast IR probe pulses described above, and the time delay between the photolysis and probe laser pulses was controlled electronically. All other aspects of the experiment remained the same.

A linear pixel to wavelength calibration of all IR absorption spectra was performed by measuring the absorption spectra of static samples such as 1,4-dioxane or cis-stilbene using the broadband IR laser pulses and the spectrometers and array detectors described above. The spectra were then placed on a wavenumber scale by direct conversion from wavelength. An IR spectrum of a static sample of each reaction mixture was also recorded using an FTIR spectrometer with 1 cm^{-1} spectral resolution both before and after 266-nm irradiation with the nanosecond Nd:YVO_4 laser for ~15 mins. From the difference between these spectra, fundamental bands of HCN (DCN) reaction product were identified in the C–H (C–D) and C≡N stretch regions centred at ~3160 cm^{-1} (2600 cm^{-1}) and 2095 cm^{-1} (1920 cm^{-1} for DCN), respectively. These band positions correspond to shifts from the wavenumbers of HCN fundamental bands in the gas-phase of ~ –48 cm^{-1} for the C–H and ~ –3 cm^{-1} for the C≡N stretch (–27 and –6 cm^{-1} respectively for DCN) in these chlorinated solvents. In our previous study,[14] the locations of the C–H vibrational hot bands of HCN were found to be separated from the respective fundamental bands by the same wavenumber interval that is observed in gas-phase experiments.[15,16] Thus, constant solvent shifts are assumed for all other transitions in the same region, such as vibrational hot bands of the same mode or combinations of the fundamental transitions with the diagonal hot bands of other vibrational modes. Anharmonicity of the modes of HCN ensured that absorption bands corresponding to vibrational ground state and vibrationally excited molecules could be distinguished in the spectra.

3. Results and discussion

Results are presented in this section in the form of time-dependent IR spectra and integrated band intensities obtained from Gaussian fits to the spectral features. The data are analysed in terms of kinetic models that describe the branching of the reaction to form HCN or DCN in specific vibrational levels, and the subsequent relaxation to the vibrational ground state by collisions with the solvent. Some of the vibrational relaxation rates, as measured by ultrafast IR pump and IR probe spectroscopy methods, were reported previously.[14] The C–H stretching region of HCN is less spectrally congested than the C–D stretching region of DCN or the C≡N stretching regions of both HCN and DCN, and therefore yields the greatest amount of information about the reaction dynamics. The HCN data are therefore presented first, followed by results for DCN, the interpretation of which is guided by the HCN experiments. Spectra obtained in the C≡N region of HCN are further complicated by overlapping bands that we assign to formation of INC (by recombination of I and CN from ICN photolysis) and CN radicals complexed to solvent molecules, and these features are also discussed.

3.1 Reactions of CN radicals with RH: the C–H stretching region

Figure 1 shows transient IR absorption spectra in the C–H stretching region of HCN products of the reactions of CN radicals with a 1.0 M solution of cyclohexane in $CHCl_3$, and 1.5 M TMS in $CDCl_3$. CN radicals were formed at time t = 0 ps by 266-nm photolysis of ICN. Analogous results were also obtained for the reaction of CN radicals with other concentrations of cyclohexane and TMS, in solution in these and other chlorinated solvents, as specified in section 2, and with neat solvent ($CHCl_3$ and CH_2Cl_2). A small number of experiments were performed for ICN and cyclohexane solutions in CH_2Cl_2 in which reaction was initiated by 255-nm UV photodissociation of ICN (with the 255-nm light generated by OPA wavelength conversion from the 800-nm fundamental). In all cases the transient spectra were very similar in appearance to the spectra presented in figure 1, and no significant differences were noted between reactions initiated by 255 and 266 nm UV pulses.

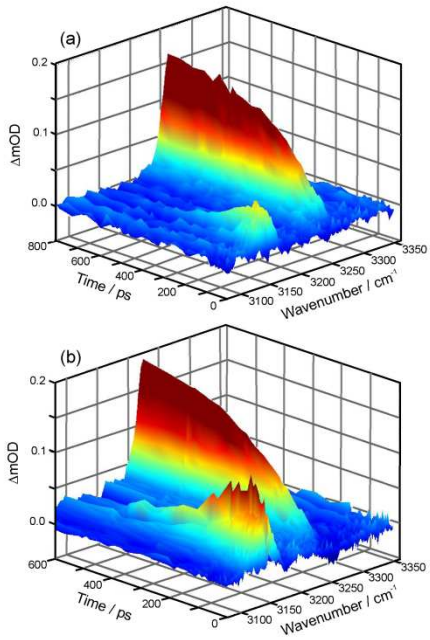

Figure 1: Time-resolved IR spectra in the C–H stretching region of HCN products of UV initiated reactions of CN radicals with (a) 1.0 M cyclohexane in $CHCl_3$; (b) 1.5 M TMS in $CDCl_3$.

The spectra show two main absorption features, centred at 3263 and 3160 cm^{-1}, which occur at the same wavenumbers as the bands observed in our previously reported IR pump-probe experiments,[14] and can be assigned to the fundamental (3_0^1) and hot band (3_1^2) transitions of the C–H stretch of HCN. Shoulders observed to the low wavenumber sides of the main bands are attributed to a progression in the HCN bending vibration (2_n^n with $n\geq1$ denoting the number of quanta of bending vibration excited) in combination with Δv_3=+1 C–H stretching bands. Equivalent combination bands for C–H stretch excitation with diagonal hot bands in the C≡N stretch are expected to arise at similar frequencies but, guided by previous gas phase studies,[17-19,22,27] and evidence from the spectra obtained in the C≡N stretching region (*vide infra*), we assume little or no excitation above v_1=0 of the C≡N stretching mode. We found no evidence for the population of HCN in the v_3=2 vibrational level, which would be observed in absorption as a band centred at ~3060 cm^{-1}. No absorption features were observed in this region above the baseline noise levels of the spectra, indicating an upper limit for HCN(002) at early times of 10% of the total HCN yield.

For the reaction of CN radicals with cyclohexane and TMS in solution in CH_2Cl_2 and $CHCl_3$, both the organic reagent and the solvent may contribute to the formation of HCN products. In transient spectra of the reaction of CN radicals with the pure solvents taken under otherwise identical experimental conditions, the maximum signal intensity of the HCN formed from reaction with the solvent does not exceed 50% of the maximum signal intensity observed in the solutions containing cyclohexane or TMS. The preferential reaction of CN with the cyclohexane or TMS solute is despite the greater concentration (by a factor of 8 or more) of the pure chlorinated solvent. Even with account taken for the greater number of possible sites for H atom abstraction for the reactions with cyclohexane and TMS, we would expect on statistical grounds that the signal intensity for the reaction with the solvent reached ~67% of the maximum intensity for reaction in $CHCl_3$ and ~133% for reaction with CH_2Cl_2; the observations may therefore reflect steric constraints on the reactions of the chlorinated solvents with CN radicals.[28] The low solubility of ICN in cyclohexane or TMS prevented study of the CN radical reactions with these organic molecules in the absence of a chlorinated solvent.

The transient spectra recorded at different time delays between UV photolysis and IR probe, and plotted on a wavenumber scale, were fitted to a set of Gaussian functions to quantify the time dependence of the intensity of the vibrational bands. The line centres of the Gaussian functions were fixed according to the assigned wavenumbers of the 3_0^1, $2_n^n3_0^1$, 3_1^2 and $2_n^n3_1^2$ bands, as described in section 2. The Gaussian line widths were assumed to be the same for all features and a value for the width was obtained from Gaussian fits to the late time (≥500 ps) spectra for which only the 3_0^1 band is observed. With this fitting procedure, we implicitly assume that the rotational motions of the HCN have thermalized through solvent friction for all time delays. In all cases, fitting incorporated six Gaussian functions corresponding to the 3_0^1 and 3_1^2 bands and $2_n^n3_0^1$ and $2_n^n3_1^2$ combination bands with n = 1 and 2 quanta of bending vibration. There was no evidence for excitation of higher numbers of quanta of the bend.[14]

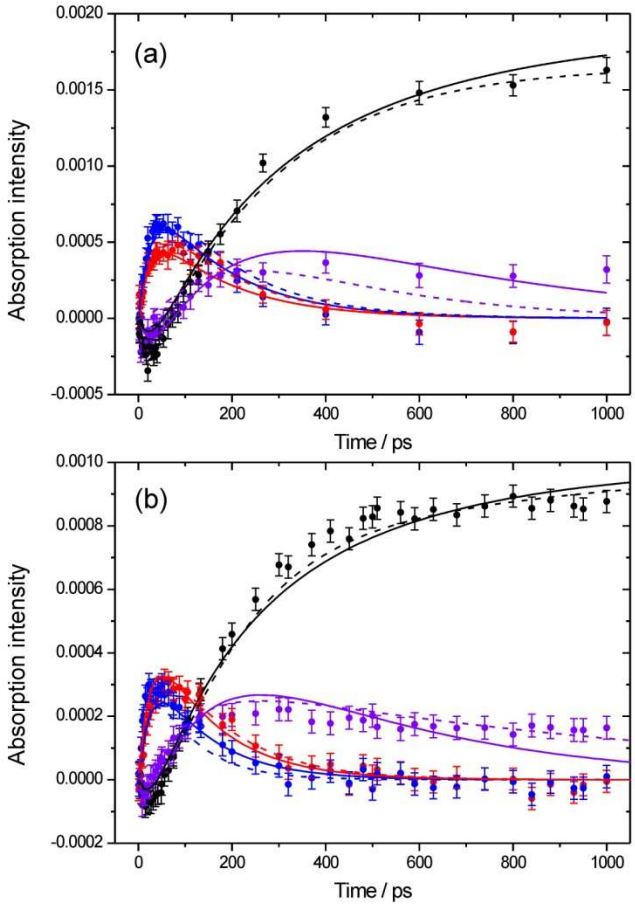

Figure 2: Time resolved integrated band intensities from C–H stretching region spectra for HCN from (a) an ICN / 1.5 M cyclohexane / CD_2Cl_2 solution; (b) an ICN / 1.5M cyclohexane / $CHCl_3$ solution. Circles are experimental measurements, with fits to model 1 (solid line) and model 2 (dashed line) as described in the text. Black is HCN(000), purple is HCN(0*n*0), red is HCN(001), and blue is HCN(0*n*1).

Examples of the time-dependence of integrated areas of the Gaussian fit functions are plotted in Figure 2. In the figure, the intensities of the bend excited combination bands with n =1 and 2 have been summed. In all cases, the maximum intensity of the $2_2^2 3_1^2$ band was not more than 50% of that of the $2_1^1 3_1^2$ band, which itself was less than 33% of the maximum intensity of the 3_1^2 band. Inspection of transient spectra such as those shown in figure 1, and the resulting time dependences of the bands potted in figure 2 shows that the 3_1^2 and $2_n^n 3_1^2$ bands grow in at early time whereas the 3_0^1 and $2_n^n 3_0^1$ bands are either absent, or negative at early times, and show subsequent growth over a longer time scale. The temporal profile of the $2_n^n 3_1^2$ band typically peaks from ~10–50 ps before the 3_1^2 band, indicating an initial bending excitation of the HCN in

addition to nascent C–H stretching motion. The 3_0^1 band becomes the sole (or predominant) feature at the longest time delays. Negative signals for the 3_0^1 and $2_n^n 3_0^1$ bands at early time are attributed to a population inversion between the v_3=0 and v_3=1 vibrational levels. The time-dependence of the IR spectra therefore provides firm evidence for reaction dynamics which preferentially form HCN vibrationally excited with one quantum of C–H stretch motion. This vibrational motion undergoes subsequent relaxation by the solvent bath to the vibrational ground state on timescales longer than 100 ps. These quantum-state specific dynamics are common to the reactions of CN radicals with cyclohexane and TMS in the chlorinated solvents, and to reactions with chloroform and dichloromethane.

The kinetics of the reaction of CN with an organic hydride molecule and the subsequent solvent induced relaxation of any vibrationally excited HCN product were modelled by adopting the reaction scheme below. Non-equilibrium molecular dynamics carried out by Glowacki *et al*.[29] highlighted a breakdown of linear response theory at short times following H abstraction, and showed that the fits to early time data may be improved by incorporating two different HCN relaxation timescales: (i) fast in-cage relaxation at short times when the HCN is in close proximity to the radical co-product; and (ii) slower relaxation of solvated HCN following diffusion away from the radical co-product. These more detailed models, which mostly improve the short time kinetic fits, are not at odds with the following general deductions about the reaction dynamics and mechanism, however. In the mechanistic scheme below, processes (1)–(4) are bimolecular chemical reactions which produce HCN in specific vibrational states, and processes (5)–(8) are state-resolved vibrational relaxation steps involving the transfer of energy to the surrounding solvent. The notation HCN($v_1v_2v_3$) specifies the number of quanta of the three vibrational modes of HCN, the C≡N stretch (v_1), the bend (v_2) and the C–H stretch (v_3). The number of quanta of bending vibration is set to be either 0 or *n* (which takes the values of 1 and 2) and the number of quanta of C–H stretch is v_3=0 or 1, consistent with the spectral assignments described above. Excitation of, and coupling to, the C≡N stretch were excluded in the model, as were other intramolecular couplings between vibrational modes which might allow, for example, relaxation of the C–H stretch into bending vibrations.

$$\mathrm{CN} + \mathrm{RH} \xrightarrow{k_1} \mathrm{HCN}(0n1) + \mathrm{R} \quad (1)$$

$$\mathrm{CN} + \mathrm{RH} \xrightarrow{k_2} \mathrm{HCN}(001) + \mathrm{R} \quad (2)$$

$$\mathrm{CN} + \mathrm{RH} \xrightarrow{k_3} \mathrm{HCN}(0n0) + \mathrm{R} \quad (3)$$

$$\mathrm{CN} + \mathrm{RH} \xrightarrow{k_4} \mathrm{HCN}(000) + \mathrm{R} \quad (4)$$

$$\mathrm{HCN}(0n1) \xrightarrow{k_5} \mathrm{HCN}(001) \quad (5)$$

$$\mathrm{HCN}(0n1) \xrightarrow{k_6} \mathrm{HCN}(0n0) \quad (6)$$

$$\mathrm{HCN}(001) \xrightarrow{k_7} \mathrm{HCN}(000) \quad (7)$$

$$\mathrm{HCN}(0n0) \xrightarrow{k_8} \mathrm{HCN}(000) \quad (8)$$

Reactions (1)–(4) and collisional relaxation steps (5)–(8) are treated as pseudo first-order processes because the organic reagent RH and the solvent are in large excess over the CN radicals and the HCN product. The time dependent IR absorption signals measured experimentally depend on: (i) time-dependent concentration of HCN in specific vibrational levels; (ii) the difference in population between the vibrational levels connected by IR transitions; and (iii) the magnitudes of the IR transition dipole moments for the spectral bands. The set of differential equations which describes the kinetics of steps (1)–(8) can be solved analytically for the time-dependence of the concentration of HCN in the different vibrational levels. Expressions for time-dependent population differences between the vibrational levels probed by IR absorption were then derived and formed the basis of simultaneous fits to the data sets such as those shown in each panel of figure 2.

In the case of the 3_1^2 and 3_0^1 vibrational bands, we simply consider the difference in the populations of the upper and lower levels of the IR transition, with the population of the level with v_2=2 set to zero because we see no evidence for absorptions from this level. The appropriate expression for the intensity of the $2_n^n 3_0^1$ band is less clear-cut, however, as contributions from levels with n = 1 and 2 quanta of bending vibration are incorporated into each population expression, and we compared fits using two models which treat the population differences differently. Model 1 assumes that the time-dependent evolutions of the populations of the bending modes are identical in

combination with both the upper and the lower C–H stretching vibrational levels, and population differences for the upper and lower levels of the $2_n^n 3_0^1$ band are incorporated accordingly. Model 2 considers the limit that the time-dependences of the populations of bending levels differ when associated with v_3=0 and 1, in which case population differences between the upper and lower levels of the $2_n^n 3_0^1$ band are not incorporated in expressions used for the fits. A ratio of 1.76 for the magnitudes of the transition dipole moments for the 3_1^2 hot band of the C–H stretch and the 3_0^1 C–H stretching fundamental was calculated by Botschwina,[30] but, as was argued previously,[14] this value was allowed to float in fits. Values in the range 1.0 – 1.2 were typically obtained, and are consistent with the relative intensities of these bands observed in IR pump and IR probe experiments. Combination bands of the C–H stretching mode with bending vibrational diagonal hot bands were assumed to have the same transition dipole moment as the pure fundamental C–H stretching bands.

The analytical expressions for time-dependent vibrational level populations and population differences were used for least-squares fits to numerous data sets of time-dependent band intensities, such as those in figure 2, to derive values for the rate coefficients $k_1 - k_8$. We previously reported use of IR-pump and IR-probe spectroscopy to determine first-order time constants for the relaxation of HCN(v_3=1) and the recovery of HCN(v=0) in $CHCl_3$, CH_2Cl_2 and $CDCl_3$ of 130±5, 144±8 and 265±20 ps, respectively,[14] and have since determined a time constant of 170±6 ps for HCN(v_3=1) relaxation in CD_2Cl_2. To constrain the fits to the current data, we fixed the rate coefficients for the relaxation of one quantum of C–H stretch (k_6 and k_7) to the reciprocal of the time constant for HCN in the appropriate solvent. In all cases the fits to Models 1 and 2 capture the main trends in the time-dependence of all data, and any minor discrepancies between the fits and the data are likely to be a result of simplifying assumptions in our reaction mechanism (e.g., omission of intramolecular vibrational redistribution processes; restriction of vibrational relaxation to single-quantum steps) and the modelling of the population differences of the IR transitions.

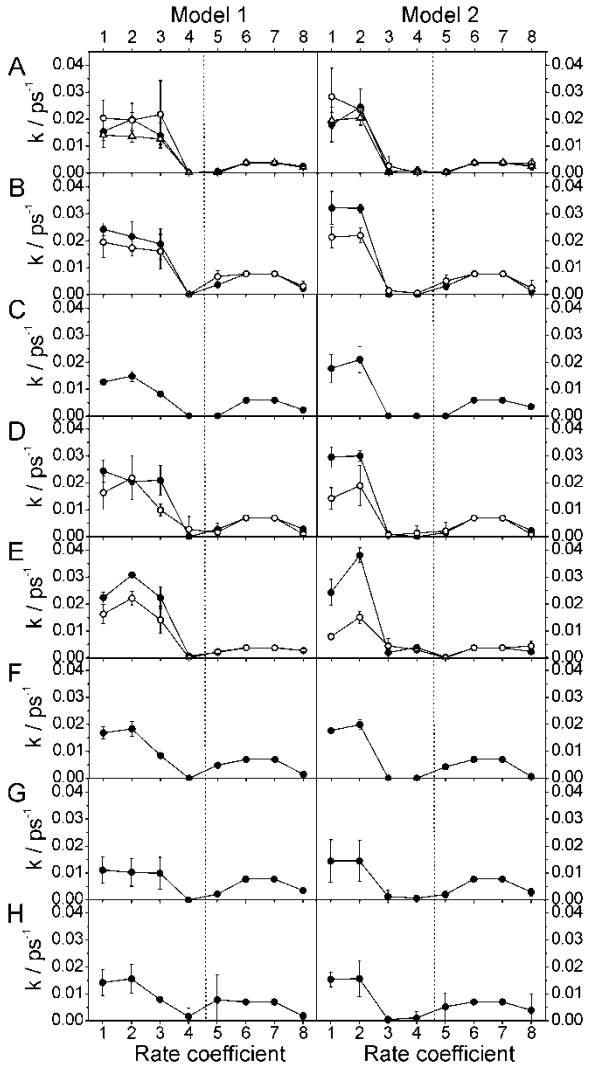

Figure 3: Rate coefficients for the reaction CN + RH → HCN + R using Model 1 (left column) and Model 2 (right column) described in the text. The first four rows are for the reactions of CN with cyclohexane in: (A) $CDCl_3$; (B) $CHCl_3$; (C) CD_2Cl_2; and (D) CH_2Cl_2. The fifth and sixth rows are for reaction of CN radicals with TMS in: (E) $CDCl_3$; and (F) CH_2Cl_2. The final two rows show results of reaction of CN radicals with chlorinated solvents: (G) $CHCl_3$; and (H) CH_2Cl_2. In panels (A)–(E), the solid circles are the results of fitting to solutions containing 1.5 M cyclohexane or TMS, as appropriate, open circles are for 1.0 M solutions, and the open triangles in (A) are for a 0.75 M solution. In (B), (C), and (E) the contributions from reaction with the solvent were subtracted prior to fitting the data. All results presented are for reactions initiated by 266 nm UV photolysis of ICN. The dashed vertical lines separate the rate coefficients for the bimolecular reactions (1-4) from those for vibrational relaxation (5-8), as defined by the kinetic scheme in the main text. The rate constants k_6 and k_7 were fixed to the measured relaxation rates of HCN(v_3=1) in the appropriate solvent,[14] as described in the text. The data presented are averages and uncertainties (1 s.d.) in the values derived from 2-6 replicate data sets.

Figure 3 compares the resulting rate coefficients derived from the two kinetic fitting models for the reaction of CN radicals with various concentrations of cyclohexane and TMS in chlorinated solvents, and the reaction of CN radicals with chloroform and dichloromethane solvents. A number of trends can be noted which are common to all reactions and chosen solvents. Firstly, the rate coefficients k_1 and k_2 for the formation of C–H stretch excited HCN products of bimolecular reaction are consistently much greater than k_4, the rate coefficient for the formation of HCN in the vibrational ground state. Secondly, the rate coefficients derived from Model 1 and Model 2 are quantitatively similar, except that the k_3 for the formation of bend excited HCN (without C–H stretch excitation) is similar in magnitude to k_1 and k_2 for Model 1, but tends to be lower in magnitude for Model 2. Thirdly, the magnitudes of k_1-k_4 tend to decrease as the concentration of cyclohexane or TMS is reduced (although this is not clear-cut for the data shown in figure 4A). The rate coefficients for bimolecular reaction k_1-k_4 were treated as pseudo first-order, in which case they should depend linearly on the concentration of the reagent RH, $k_i = k_{bm,i}[RH]$, where $k_{bm,i}$ is the second-order rate coefficient for the i^{th} reaction and RH is cyclohexane, TMS or the chlorinated solvent. This behaviour is roughly followed. The vibrational relaxation rate coefficients are independent of the concentration of the cyclohexane or TMS, as might be expected for removal of vibrational energy being dominated by coupling with the solvent. The rate coefficients for CN reaction with $CHCl_3$ and CH_2Cl_2 can be estimated from the sums of k_1–k_4 (using average values from fits to models 1 and 2) to be $(2.50 \pm 1.41) \times 10^9$ mol^{-1} dm^3 s^{-1} and $(2.30 \pm 0.77) \times 10^9$ mol^{-1} dm^3 s^{-1} respectively. These reaction rate coefficients are a factor of ~4.5 ($\pm$ 2.5) times larger than reported values for the gas-phase reactions at 298 K.[31]

The values of k_1–k_4 can be interpreted to be proportional to the reactive branching to form nascent HCN(0n1), HCN(001), HCN(0n0) and HCN(000) products, respectively. Within the uncertainties of these measurements, the branching ratios are consistent for the different reactions investigated of CN with cyclohexane, TMS, $CHCl_3$ and CH_2Cl_2 and do not depend on the choice of solvent. Reactions with the solvent are, however, slower than those with cyclohexane and TMS. Approximate branching ratios, HCN(0n1): HCN(001): HCN(0n0): HCN(000), for the partitioning of energy into the vibrational states of the nascent HCN reaction product of 0.33:

0.33: 0.33: 0.01 are derived from Model 1, with Model 2 resulting in ratios of 0.4: 0.4: 0.1: 0.1 (both distributions are normalized to sum to unity). Thus, the rate coefficients derived from both Model 1 and Model 2 provide evidence that all reactions investigated preferentially (~66–80%) form HCN with one quantum of C–H stretch excitation, and we deduce that vibrational excitation accounts for ~30-35% of the energy available to products. The predominant (~90-99%) source of HCN(000) is through vibrational relaxation of nascent, vibrationally excited products by coupling to the solvent.

3.2 Reactions of CN radicals with RH: the C≡N stretching region

Similar measurements to those described in section 3.1 were performed in which the HCN product of reaction of CN with cyclohexane or TMS was instead probed in the C≡N stretching region at ~2100 cm^{-1}. Figure 4 shows a representative time-dependent transient spectrum for the reaction of CN radicals with 1.5-M cyclohexane in solution in chloroform, and analogous measurements were also performed for the reaction of CN with 1.5 M cyclohexane in $CDCl_3$ and CH_2Cl_2, the reaction of CN with 1.5 M TMS in $CDCl_3$ and CH_2Cl_2, and the reaction of CN with neat CH_2Cl_2 and $CHCl_3$ solvents. The resulting spectra were all qualitatively similar to the transient spectra presented in figure 4, and show three positive absorption features which grow in with time. A weak feature is centred at 2037 cm^{-1}, and two stronger features arise with centres at 2065 and 2094 cm^{-1}. In addition, a negative feature is observed at 2176 cm^{-1} (not shown in the figure) which shows almost no time dependence, and which is identified as a photolysis-laser induced bleach of ICN.[32] In experiments with UV pumping of mixtures of ICN in $CDCl_3$, for which no hydride species are present, the absorption features centred at 2037 and 2065 cm^{-1} remain, but the band at 2094 cm^{-1} is lost. We assign this latter feature as the 1_0^1 band of HCN(000), which is consistent with FTIR spectra of reaction samples and our previous IR pump – IR probe experiments.[14] The feature at 2037 cm^{-1} is very close in wavenumber to the fundamental vibrational band of CN in the gas phase,[32] and we assign it to free CN radicals or, more likely, to CN radicals that are weakly complexed to the chlorinated solvent molecules.[11,12] The band at 2065 cm^{-1} is assigned to the N–C stretch of INC, based on reported band frequencies from matrix isolation spectra.[32] We saw no

evidence for the formation of ClCN, which would be expected to absorb at ~ 2215 cm^{-1}.[32] Hot-bands of HCN involving the C≡N stretching mode, or the C–H stretch in diagonal combinations with the fundamental C≡N stretching transition, are expected to fall under or close to the CN and INC features and could not be distinguished. For example, absorption via the $1_0^1 3_1^1$ combination band should be evident at early times because of nascent excitation of the C–H stretching mode, but this band is expected to arise at ~2079 cm^{-1} and is difficult to extract from between the neighbouring INC and HCN(000) features, although there is evidence from spectra for its presence. The band at 2094 cm^{-1} may incorporate overlapping contributions from the $1_0^1 2_n^n$ bending progression, which has expected anharmonic spacings of only ~3 cm^{-1} and could not be resolved experimentally.

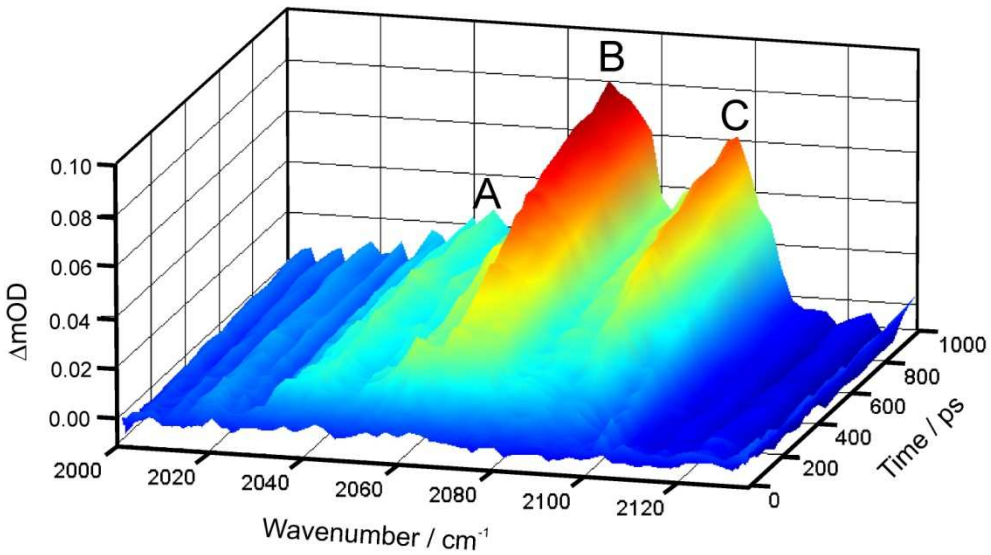

Figure 4: Time-dependent IR spectra in the C≡N stretching region of HCN, for reaction of CN radicals with cyclohexane (1.5 M) in $CHCl_3$. The zero of time is defined by the UV photolysis of ICN to generate CN radicals. Features centred at 2037 cm^{-1} (A), 2065 cm^{-1} (B) and 2094 cm^{-1} (C) are assigned, respectively, to CN radical complexes with the solvent, the N-C stretch of INC, and the fundamental C≡N stretching band of HCN.

The time dependence of each of the spectral features was quantified by simultaneous least squares fitting of Gaussian functions to spectra at all time steps. Within the signal-to-noise levels of the measurements, the ICN bleach feature showed no time dependent recovery, and was not analysed further. The Gaussian function centres were fixed at the central frequencies of the spectral bands and the widths were

constrained to a constant value. Figure 5 shows the resulting time dependences for the CN, INC and HCN(000) features for the reaction of CN with 1.5 M cyclohexane in $CHCl_3$. The CN and INC bands show fast rise times (with time constants < 30 ps) and appear before the 1_0^1 band of HCN, which exhibits an induction period of up to 50 ps suggesting the HCN(000) arises – at least in part – following vibrational relaxation.

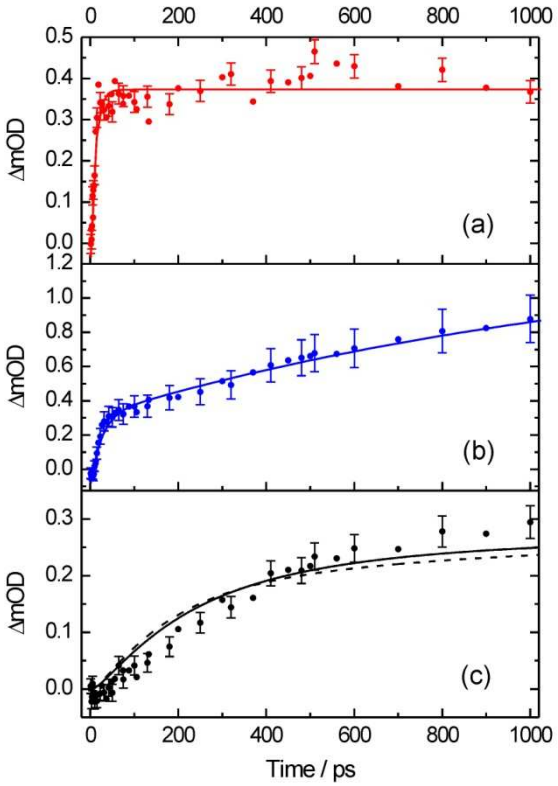

Figure 5: Time dependence of the spectral bands shown in figure 4 and centred at (a) 2037 cm^{-1}, (b) 2065 cm^{-1} and (c) 2094 cm^{-1}. These bands are respectively assigned to CN complexes with solvent, INC and HCN(00), all of which result from UV photolysis of ICN in a solution of 1.5 M cyclohexane in $CHCl_3$. The experimental data are shown by circles and the lines in panels (a) and (b) are fits to the data, as described in the text. In (c) the contribution to the HCN signal from the reaction with the solvent has been subtracted. Simulations of the expected time-dependence of HCN(000) data using rate coefficients derived from analysis of time-dependent band intensities in the C–H stretching region are shown as the solid (model 1 – see text) and dashed (model 2) black lines.

In this regard, the behaviour of the 1_0^1 band is similar to that of the 3_0^1 band in the C–H stretching region. The behaviour of the upper state of the IR transition differs for the two features, however, with the most notable difference being the absence of (or, at most, only weakly evident) negative going signal in the 1_0^1 band at the earliest times (<200 ps). We take this observation as evidence that the HCN(100) level is not

substantially populated by the reaction. In the kinetic model described in the previous section, we assumed that the C≡N stretching vibration of HCN is not excited above its zero-point level following H-atom abstraction by CN radical. To test this assumption further, the rate coefficients presented in Figure 3, which result from the kinetic fits to the C–H region data, were used to simulate the kinetics of the 1_0^1 band using a model in which the HCN(100) level is unpopulated at all times. The results of such simulations, using the rate coefficients derived from kinetic models 1 and 2, are in reasonable agreement with the experimentally observed time-dependent band intensities, as shown in figure 5(c).

The data shown in figure 5 are for reaction in solution in $CHCl_3$, but very similar behaviour was observed in $CDCl_3$. In solution in $CDCl_3$, the relaxation time constants for C≡N and C–H stretching excitation were measured by IR-pump and IR-probe experiments to differ by a factor of ~two (122 ± 20 and 265 ± 20 ps respectively).[14] For reactive production of HCN in $CDCl_3$ solution, the temporal rise in 1_0^1 band intensity from 200 ps onwards is much better modelled using a time constant $\tau = 265$ ps than $\tau = 122$ ps, providing further evidence that the HCN(000) probed via this band is formed by relaxation of C–H (and not C≡N) stretch-excited products. The transient IR spectra for the C≡N region of HCN are therefore consistent with the picture of the reaction dynamics deduced from the results for the C–H region in which the C–H stretching and bending modes of HCN are excited, with the C≡N stretch remaining an unexcited spectator mode.

The CN complex and INC spectral features show very fast initial rises followed either by an extended period of constant absorption (CN) or a slow further rise (INC). The CN data shown, and those obtained for other solutions studied, can be fitted to a single exponential function, as shown by the solid line in figure 5(a), from which an initial rise time constant in the range $\tau = 8 - 26$ ps is derived, with no particular dependence on whether the co-reagent present is cyclohexane, TMS or pure solvent, or the choice of chlorinated solvent. INC will form by the recombination of I and CN after rotation of the CN radical, which is known to be produced with high angular momentum at short times in solution following ICN photodissociation.[25,26] This recombination pathway has been identified previously both in solution (by time-

resolved UV/vis spectroscopy) and within rare gas matrices after photodissociation of ICN at 266 nm.[33,34] For our data in various solvents, the INC band intensities fit well to a bi-exponential rise, with two distinct time constants of τ_1 = 11 – 22 ps and τ_2 > 500 ps, as shown in figure 5(b). The fast initial formation of INC occurs on similar timescales to that of the CN-complex formation, and is attributed to geminate recombination within the original solvent shell. The longer timescale growth of INC is indicative of diffusive recombination after escape from the initial solvent cage. The amplitude of the slow signal is typically more than twice the amplitude of the fast signal, irrespective of the solvent used. The fits therefore indicate that ≤1/3 of the INC is formed by recombination within the initial solvent cage, for all the chlorinated solvents used. Time constants for INC and CN-solvent complex formation and estimated fractions of INC formation by diffusive recombination in a variety of solutions are displayed in Table 1. The data suggest that in-cage recombination to form INC is marginally more significant in $CHCl_3$ (and $CDCl_3$) than in CH_2Cl_2.

Solvent	Organic reagent	INC			CN-solvent complex
		τ_1 / ps	τ_2 / ps	Diffusive recombination fraction	τ / ps
$CDCl_3$	1.5 M c-C_6H_{12}	21.0 ±8.3	524 ± 213	0.74 ± 0.08	8.4 ± 6.8
$CDCl_3$	Solvent	21.9 ± 7.3	661 ± 211	0.73 ± 0.19	26.2 ± 10.8
$CHCl_3$	1.5 M c-C_6H_{12}	20.2 ± 4.5	1095 ± 359	0.72 ± 0.04	14.6 ± 6.5
$CHCl_3$	Solvent	20.9 ± 5.4	> 2000	0.62 ± 0.19	17.1 ± 3.3
CH_2Cl_2	1.5 M c-C_6H_{12}	11.8 ± 5.6	757 ± 276	0.80 ± 0.03	7.4 ± 2.4
CH_2Cl_2	1.5 M TMS	17.9 ± 3.8	> 2000	>0.9	14.4 ± 3.5
CH_2Cl_2	Solvent	18.1 ± 4.5	> 2000	0.86 ± 0.06	14.5 ± 3.0

Table 1: Time constants obtained from bi-exponential and single exponential fits respectively to the time-dependence of the INC and CN-solvent complex IR absorption bands. Values are presented for UV photolysis of 0.14 M ICN solutions in the solvents indicated, either in the presence or absence of the organic co-reagent cyclohexane or TMS. The estimated fractions of INC formed by diffusive recombination are also listed.

To investigate further the lifetimes of the CN and INC species, we used the nanosecond experimental setup described in Section 2 to vary the time delay between UV photodissociation and IR detection over the extended range of 1 – 200 ns. The INC was observed to persist across this full range of time delays. The CN feature, however, was not observed in these experiments, suggesting a lifetime of only a few nanoseconds. In the gas phase, ICN is ~28.3 kcal mol^{-1} more stable than INC, with a barrier to isomerisation from INC to ICN of 18 kcal mol^{-1}.[35] Thus, at thermodynamic equilibrium, we expect a negligible fraction of the INC isomer. However, at the earliest times of recombination of I and CN, either ICN or INC can form, and rapid relaxation in solution may trap the metastable INC isomer. We see no evidence for the spectral signature of INC in FTIR spectra of static reaction samples after ~15 mins UV irradiation, which is consistent either with the isomerisation reaching an equilibrium distribution under these static conditions, or reactive loss of any INC formed. As was noted earlier, the recovery of ICN following initial photodissociation is not observed in our experiments, but the IR intensity of the C≡N stretching fundamental vibrational band of ICN has been experimentally determined to be a factor of 117 ± 10 lower than for INC.[35] If the population of ICN formed by recombination of I and CN on the timescales of the ultrafast experiments is comparable to that of INC, only a ~0.5% change in the ICN bleach intensity is therefore expected. Development of pink coloration to the solutions after several minutes of UV irradiation is also indicative of production of I_2 from liberated I atoms.

3.3 The reaction of CN radicals with d_{12}-cyclohexane

Transient IR spectra of DCN formed from reaction of CN radicals with d_{12}-cyclohexane in solution in $CHCl_3$ were obtained in both the C≡N (~1920 cm^{-1}) and C–D (~2600 cm^{-1}) stretching regions. We retain these convenient labels for the vibrational modes ν_1 and ν_3, but note that the two stretching modes of DCN are not as localised in the separate bonds as is the case for HCN. The C≡N stretching bands of DCN do not suffer the interferences from INC and CN bands discussed in the context of HCN spectra because of the shift of the C≡N stretching mode to lower wavenumber. The DCN spectra were accumulated over time intervals between the UV photolysis laser and the broadband IR probe laser of 1 – 1300 ps, and show

considerable variation with time delay. Bands were assigned using spectroscopic data for gas-phase DCN, shifted to lower wavenumber to account for solvent effects. The shifts applied in the C≡N and C–D regions were, respectively, –6 and –27 cm^{-1} and were determined for the fundamental bands and then applied to all other bands in the same spectral region. In both the C≡N and C–D region spectra, there is evidence for considerable vibrational excitation of the nascent products, with many similarities and some subtle differences to what was observed for reactions producing HCN. Analysis of the DCN data is complicated by considerable spectral congestion and some overlapping solvent bands. Nevertheless, time dependent spectra are presented here with proposed assignments and are analysed to derive information on the kinetics of formation of vibrationally excited DCN and its vibrational relaxation.

3.3.a Spectra of DCN in the C≡N stretching region

A sequence of broadband IR spectra of DCN formed from reaction of CN with d_{12}-cyclohexane (1.5 M) in $CHCl_3$ at wavenumbers around 1920 cm^{-1} (the C≡N region) is shown in figure 6, and the combs above the spectra indicate expected band positions. In this region, the anharmonic coupling of the bending modes to C≡N stretching modes causes progressions of vibrational hot bands diagonal in the bending mode to extend to higher wavenumber. There is considerable overlap of spectral bands, but features can plausibly be assigned to the following transitions: $1_0^1 2_n^n$ (n≥0, with the n=0 feature dominating at later times), $1_0^1 2_n^n 3_1^1$, $1_1^2 2_n^n$, and perhaps also $1_2^3 2_n^n$, $1_1^2 2_n^n 3_1^1$ and $1_0^1 2_n^n 3_2^2$. The interpretation is complicated by the presence of structure remaining in the spectra from transient features caused by weak solvent bands, and a solvent spectrum is also shown in figure 6 to indicate the locations of these solvent absorptions. The spectra show a clear evolution with increasing time delay from features at lower wavenumber towards intermediate and higher wavenumber, suggesting formation of DCN with substantial vibrational excitation, and relaxation to lower levels, and ultimately the vibrational ground state by loss of energy to the solvent. The vibrational excitation appears to be in all three modes at early times, with up to 2 quanta of C–D stretch, 2 – 3 quanta of bending excitation, and some DCN(1n1) products exhibiting simultaneous excitation of both stretching modes.

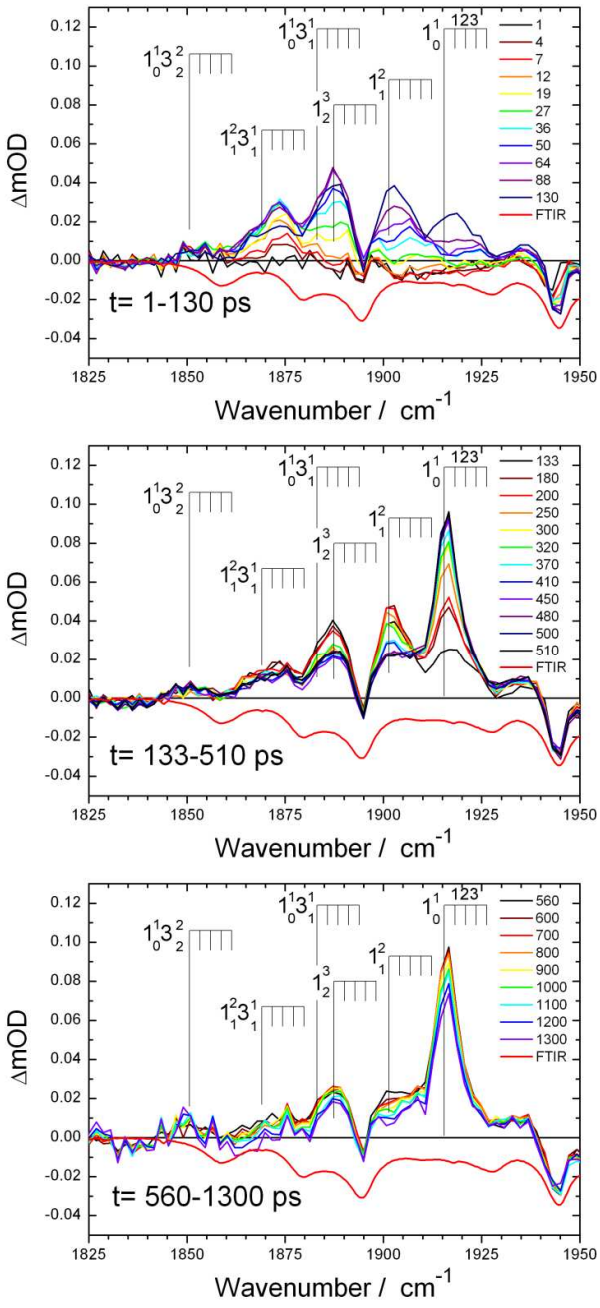

Figure 6: Transient IR spectra in the C≡N stretching region for reaction of CN radicals with 1.5 M *c*-C_6D_{12} in $CHCl_3$. The three panels show spectra for pump – probe laser delays in the range 1 – 130 ps (top), 133 – 510 ps (middle) and 560 – 1300 ps (bottom), with individual time delays (in ps) indicated in the inset keys. The combs indicate possible spectral assignments, with the ticks representing diagonal progressions in the bending vibrational mode v_2 which extend to higher wavenumber as the number of quanta of bend increases. The red lines are inverted and scaled FTIR spectra of a *c*-C_6D_{12} solution in $CHCl_3$ to show the positions of interfering weak solvent and co-reagent bands. An animated version of this figure is provided in Supplementary Information.

Time-dependences of selected spectral features are shown in figure 7, and were obtained by fitting Gaussian functions of fixed width located at the expected positions of $\Delta v_1 = +1$ transitions originating from the vibrational levels (000), (010), (100), (001), and (101) to derive integrated areas of each band. An alternative fit included three further Gaussian functions centred on features assigned to absorption from the (110), (011) and (111) levels to reduce the fit residuals. There was not a significant change in the derived time dependences of the band intensities, but indications of overlap of the Gaussian fit functions encouraged use of the smaller number.

As is evident in figure 7, all the features in the spectrum except the bands assigned to the 1_0^1 and $1_0^1 2_1^1$ transitions (corresponding to detection of DCN(000) and (010)) show fast rises and decay towards the baseline level at longer time delays. That some of the data sets do not decay fully to baseline reflects the weak signal levels and incomplete background subtraction because of overlapping solvent bands. The features assigned to possess greater amounts of vibrational excitation show the fastest initial rises, whereas those corresponding to lower vibrational levels exhibit induction periods before the onset of growth, and in some cases weakly negative intensities suggest greater population in the upper of two levels connected by a vibrational spectral transition. The 1_0^1 band grows in over several hundred picoseconds before reaching a constant value, which is indicative of its formation primarily by vibrational relaxation of nascent, internally excited DCN molecules. The shoulder to the high wavenumber side of this feature, assigned to absorption by DCN(010) products, also does not decay to zero intensity at long times. The apparent extended lifetime of DCN(010) may be a consequence of stepwise relaxation of vibrationally excited DCN (either through solvent collisions or IVR) that repopulates this lowest frequency mode over the timescale of the measurements, or our data may indicate that relaxation of the DCN(010) level to the (000) ground state is slow. Alternatively, the long-time behaviour of this shoulder may result from a baseline shift in the spectra because of a broad underlying solvent feature evident in figure 6 that is not completely removed by our baseline subtraction procedures. Bands assigned to possess a quantum of ν_3 (C–D) excitation peak before those with no excitation in this mode, even if the DCN is otherwise (e.g. C≡N stretch) excited.

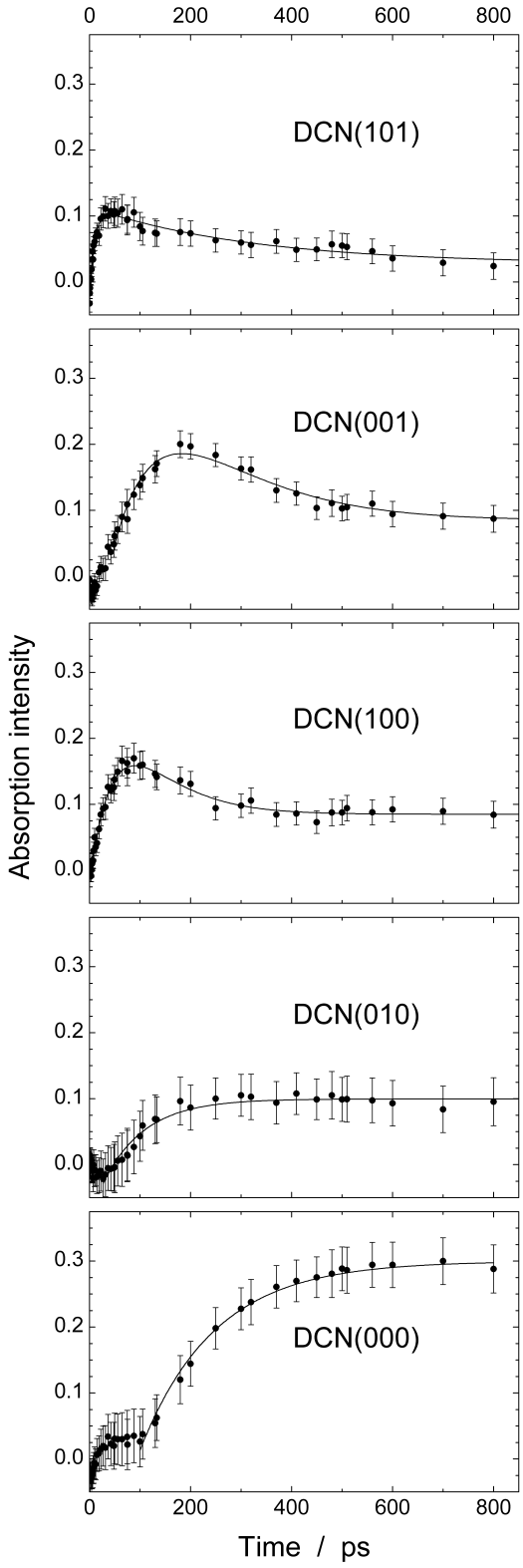

Figure 7: Time-dependence of regions of the spectra shown in figure 6 that are assigned to absorptions from DCN(101), (001), (100), (010) and (000). The solid lines are fits to bi-exponential growth and decay (top three panels) or single exponential growth (bottom two panels) functions, as discussed in the text.

A fit of the time-dependent band intensities to a kinetic model that accounts for reactions to form nascent DCN(0n0), (0n1), (1n0) and (1n1) levels, together with vibrational relaxation steps, and that allows for population differences between levels connected by IR absorptions, requires evaluation of a large number of rate coefficients. IVR, which might couple energy from one DCN mode to another, may also merit inclusion in a full model. Such full kinetic schemes rapidly become too intractable for sensible analysis of the available data, and we therefore adopted a more approximate quantification of the rates of formation and loss of DCN in individual ($v_1v_2v_3$) levels. For all bar DCN(000) and (010), the band intensities show a rise and then a decay with time, and we fitted these to a standard model for exponential growth and decay, with a time offset of up to ~45 ps to account for the delayed onset of growth of signals. Single exponential growth functions were used to parameterize the time-dependence of the DCN(000) and (010). The results of these fits are shown in figure 7 and Table 2. We note, however, that this simplified fitting cannot account for the first 30 - 40 ps of the integrated absorption signals, which exhibit induction periods that can include negative going features attributed to population inversions. We have discussed a more complete treatment of such early time data elsewhere,[29] and argued that vibrational relaxation dynamics within the initial solvent cage, with the DCN in close proximity to the *c*-C_6D_{11} radical co-product, leads to a breakdown of linear response type behaviour. In this case, the model of the relaxation kinetics needs to be modified to incorporate diffusion out of the initial solvent cage into bulk solution, and must incorporate distinct relaxation behaviours in the two different microscopic environments.

3.3.b Spectra of DCN in the C–D stretching region

The C–D stretching region also suffers from spectral congestion, as figure 8 shows. Again, combs above the spectra indicate the expected positions for the fundamental 3_0^1 band, hot bands of this mode, and various combination bands that incorporate a Δv = +1 transition in the C–D stretching mode with diagonal hot bands in the bending and C≡N stretching modes. Definitive assignments are not possible, because of the overlap of spectral features, but the proposals are consistent with the assignments for the C≡N spectral region, showing up to 2 quanta of excitation of the C–D stretch, 2

quanta of the C≡N stretch and extensive ($n \leq 3$) bending excitation in the nascent DCN reaction products. We note that the spectral overlap, and the substantial internal excitation of the DCN, raise questions about the assignment by Raftery *et al*. of a transient IR absorption feature they observed at 2555 – 2575 cm^{-1} from the CN + $CDCl_3$ reaction to DCN excited simply with one quantum of C–D stretch.[8]

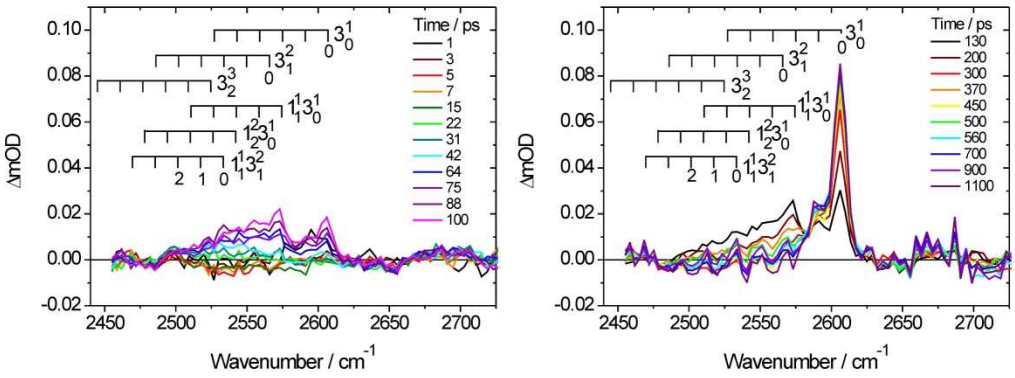

Figure 8: Transient IR spectra in the C-D stretching region for reaction of CN radicals with 1.5 M *c*-C_6D_{12} in $CHCl_3$. The left hand panel shows short time pump – probe laser delays in the range 1 – 100 ps, with the 130 – 1100 ps time delays plotted in the right hand panel. The combs indicate possible spectral assignments, with the ticks representing diagonal progressions in the bending vibrational mode v_2. An animated version of this figure is provided in Supplementary Information.

Figure 9 displays the time dependences of integrated intensities of selected features from the spectra in figure 8, obtained using a fit of 8 Gaussian functions of fixed width centred at the expected wavenumbers of bands with $\Delta v_3 = +1$ originating from DCN(000), (010), (100), (110), (001), (011), (101) and (111) levels. Alternative use of 5 fit functions at wavenumbers corresponding to transitions from the (000), (010), (100), (001) and (101) levels (as employed in the C≡N region analysis in the preceding section) made little difference to observed time dependences, but did increase the residuals from the fits. The features assigned as vibrationally excited DCN decay towards the baseline level after a few hundred picoseconds, whereas the fundamental 3_0^1 band grows to a maximum level on this timescale and maintains this absorption for more than 1000 ps. The shoulder on this band assigned as the $2_1^1 3_0^1$ band also appears to maintain above-baseline absorption over this timescale, much as was observed for DCN(010) data in the C≡N spectral region (see section 3.3.a). As

was noted earlier, persistence of absorption intensity from bend-excited DCN may be a consequence of stepwise decay of more highly vibrationally excited DCN down through a ladder of other vibrational levels to the v_2=1 level, or slow relaxation of DCN(010).

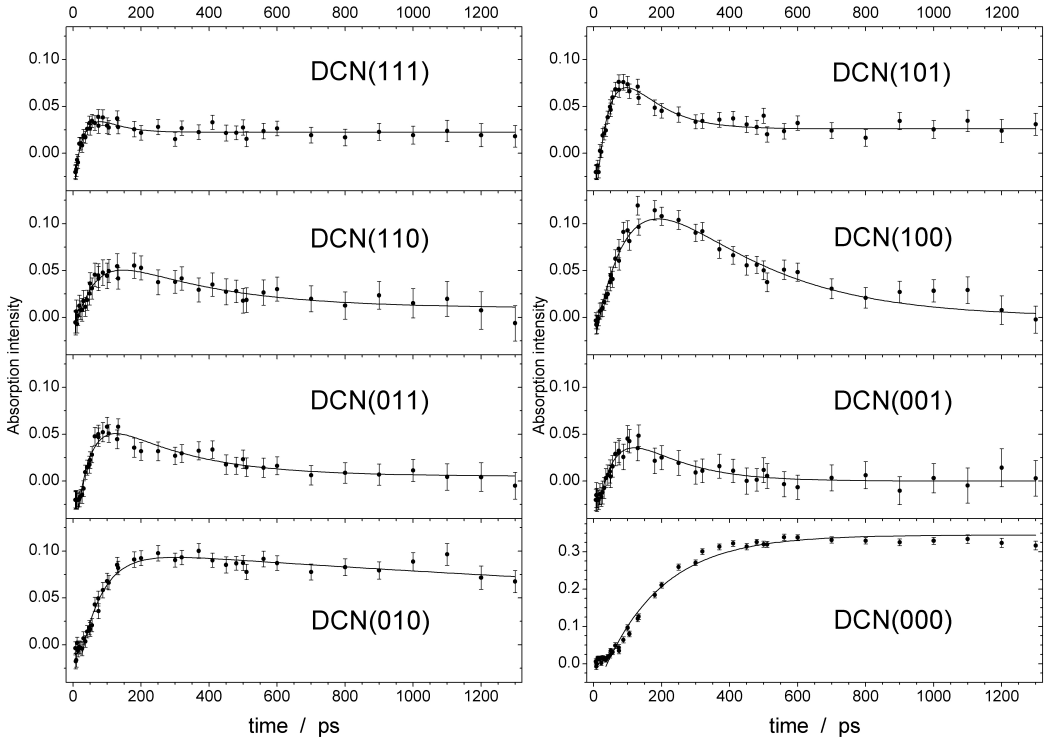

Figure 9: Time-dependence of regions of the spectra shown in figure 8 that are assigned to absorptions from DCN(000), (010), (100), (110), (001), (011), (101) and (111). The solid lines are fits to a bi-exponential growth and decay function, or a single exponential growth in the case of DCN(000).

As was the case for C≡N spectral region data, we observe the general trend that bands assigned to DCN with greater vibrational energy content – particularly those with a quantum of C–D stretch excitation – peak at earlier times than bands originating from lower energy vibrational levels. All the bands show short induction periods before the onset of growth, and this period is shorter for more highly vibrationally excited products. Both these observations are consistent with preferential formation of vibrationally excited DCN from the chemical reaction, and relaxation by loss of energy to the solvent being the main route to DCN(010) and DCN(000) molecules. They also hint at formation of DCN formed in vibrational levels higher than (101). The data plotted in figure 9 and the time constants in table 2 further indicate that bands associated with a quantum of v_3 (C–D stretching) excitation arise more rapidly

and peak at earlier times than those originating from DCN with a quantum of ν_1 (C≡N) stretching excitation. This suggests some population of ν_1-excited molecules by IVR or collisional relaxation of DCN excited in the higher frequency ν_3 mode.

As was the case with analysis of the C≡N region data (section 3.3.a), fits of intensities of spectral features to bi-exponential growth and decay functions, with an initial time offset, provide a crude quantification of the time-dependences of the DCN($\nu_1\nu_2\nu_3$) reaction products. The outcomes of such fits are shown in figure 9 and table 2, and time constants for rise and decay of absorption features associated with the various DCN vibrational levels are broadly consistent from the analysis of data for the two spectral regions. In the Supplementary Information, fits are presented to a more complicated model that may apply if, as suggested earlier, relaxation of excitation in the bending mode is slower than, and hence can be decoupled from, relaxation of the two stretching modes. This model does not, however, incorporate possible couplings between the ν_3 and ν_1 modes as discussed above.

($\nu_1\nu_2\nu_3$)	ν_1 (C≡N)		ν_3 (C–D)	
	τ_1 / ps	τ_2 / ps	τ_1 / ps	τ_2 / ps
(000)	147 ± 5	–	181 ± 20	–
(010)	82 ± 8	–	73 ± 19	4400 ± 2000
(100)	127 ± 90	175 ± 123	92 ± 23	261 ± 91
(110)	–	–	71 ± 23	211 ± 144
(001)	56 ± 26	78 ± 41	39 ± 18	295 ± 188
(011)	–	–	28 ± 14	454 ± 297
(101)	17 ± 5	104 ± 29	48 ± 20	112 ± 93
(111)	–	–	28 ± 9	315 ± 267

Table 2: Time constants derived from bi-exponential growth and decay fits (τ_1 and τ_2), or single exponential growth (τ_1 only), to the time dependences of bands shown in figures 7 and 9. For the ν_3 region data, values are averages of fits to 3 data sets, with uncertainties reported as 1 SD. For the ν_1 region data, time constants are reported from fits to one data set and uncertainties are the standard error from the fit. Analysis of a second data confirmed the values reported, but with greater fitting uncertainties.

3.4 Comparison of HCN and DCN results from CN radical reactions

Although the DCN and HCN data have much in common, with clear evidence for the nascent products being formed with significant amounts of vibrational excitation, there are some subtle differences. Most notably, the HCN data showed no strong evidence of C≡N stretching excitation, and we described the C≡N bond as a spectator to the CN + RH → HCN + R reactions. We could not observe bands indicative of C–H stretching excitation above the v_3=1 level. For CN + RD → DCN + R reactions, however, we have presented spectroscopic evidence both for C≡N mode excitation, and (tentatively) up to 2 quanta in the C–D stretching mode. These observations in part reflect the differences in the character of the stretching vibrations of HCN and DCN, as well as the greater energy gap between v_3 vibrational levels in HCN. In neither case, however, is the maximum vibrational level populated limited by the available energy of the reaction. Indeed, the fraction of the total available energy becoming vibrational excitation of the HCN at early times is ~30 %. While DCN does show excitation in both stretching modes, at early times the C–D stretching motion is more significant.

3.5 Comparison to CN radical reactions in the gas phase

Jackson and co-workers[19,22] and Macdonald and co-workers,[17,18,27] used IR chemiluminescence and IR diode laser absorption spectroscopy methods respectively to quantify the extent of vibrational excitation of HCN from reactions with small alkanes in the gas phase. Excitation of the C–H stretching and bending modes can be attributed, respectively, to an early transition state and a flat bending potential in its vicinity.[14,36] These previous experimental studies did not, however, include the cyclohexane and TMS reaction partners studied in the current work, nor reactions to form DCN. The broad conclusions from the gas-phase studies are that the HCN products were formed with greater vibrational excitation of the bending and C–H stretching modes than we observe for reactions in solution. This may be a consequence of slightly lower reaction exothermicities for our chosen systems,[36] or may reflect a change in the energy surface governing chemical reaction in the

presence of a solvent. In addition, solvent friction over the course of the reaction may remove excess energy from the internal motions of the reaction products. We reserve the details of an extensive computational study of the gas and condensed phase dynamics of CN radical reactions to another publication, in which we consider the effects of the solvent on the reaction energy landscape, location of the transition state, and nuclear dynamics.[36] The general conclusions, however, from computer simulations of the reaction of CN radicals with cyclohexane in CH_2Cl_2, are that the free energy profile for the reaction, and hence the chemical dynamics, are not significantly changed by the presence of the chlorinated solvent.[14,36] This deduction relates in part to the choice of a weakly interacting solvent as the liquid medium in which to study the chemical reaction dynamics, but nevertheless leads to the conclusion that the dynamics are surprisingly gas-phase like at short times within the relatively dense and highly collisional environment of a liquid bath.

4. Conclusions

Experimental data for the dynamics of reactions of CN radicals with cyclohexane or TMS in solution in $CHCl_3$, CH_2Cl_2, $CDCl_3$ and CD_2Cl_2, and CN reactions with d_{12}-cyclohexane in $CHCl_3$ were obtained using transient IR absorption spectroscopy with picosecond time resolution. Similar spectroscopic data were collected for reactions of CN with the chlorinated solvents as a by-product of these experiments. The exothermic H(D)-atom abstraction reactions are characterized by an attractive PES with an early (variational) transition state for isolated collisions in the gas-phase, and, in accord with expectations from the Polanyi rules, the HCN (DCN) products are substantially vibrationally excited in the C–H (or C–D) vibrational mode. Bending excitation also results from the nuclear dynamics over a PES in which extensive deviations are possible from the minimum energy collinear N≡C–H– geometry at the transition state.[14]

Remarkably, many features of these dynamics persist for reactions in the room temperature bulk liquid solvents, despite the very short (sub-ps) time intervals between solvent-solute collisions. In particular, for both CN + cyclohexane and CN + TMS reactions, we observe a population inversion in the nascent C–H stretching

mode of HCN at early times, with the HCN most likely to be formed with one quantum of C–H stretching excitation and 0, 1 or 2 quanta of bending excitation. The highest vibrational level observed spectroscopically corresponds to HCN(021). Vibrational relaxation by coupling to modes of the solvent bath is the main route to production of ground vibrational level HCN(000) and occurs with solvent-dependent time constants in the range 130 – 270 ps. No significant differences are observed for primary and secondary H-atom abstraction from TMS and cyclohexane respectively. Similar behaviour is observed for DCN from reaction of CN radicals with perdeuterated cyclohexane. Although congestion in spectra obtained in the regions of the C–D and C≡N stretching modes prevent definitive assignment of the populated vibrational levels and the branching into these levels, we present evidence for formation of DCN with both one quantum of both ν_1 (largely C≡N stretching) and ν_3 excitation. Analysis of the time-dependence indicates a preference for formation of the more highly vibrationally excited levels, and C–D stretch excitation, with subsequent relaxation by solvent coupling, is the main route to DCN in its vibrational ground state.

IR spectra obtained in the C≡N stretching region of HCN show additional transient features that we assign to formation of CN-solvent complexes, and to recombination of I atoms and CN radicals (from UV photolysis of ICN) to form INC. Both species form rapidly, with time constants of < 30 ps that do not depend strongly on the choice of chlorinated solvent.

The experimental data, and computational studies reported elsewhere, indicate that the dynamics of CN radical reactions with organic molecules in solution in the common chlorinated solvents chloroform and dichloromethane retain many of the known features of the reactions under single collision conditions in the gas phase. The solvent makes only minor modifications to the free energy surface for the reaction and, at short times, exerts few constraints on the nuclear dynamics. Whether such behaviour persists for other classes of solvent, and for other chemical reactions is the subject of ongoing investigations.

Acknowledgements

The measurements were carried out at the Central Laser Facility, Rutherford Appleton Laboratory, with financial support for the ULTRA laser facility from STFC and BBSRC (STFC Facility Grant ST/501784). Funding for the Bristol group was provided by the EPSRC Programme Grant EP/G00224X. Valuable discussions with Dr D.R. Glowacki and Profs J.N. Harvey and M.N.R. Ashfold (University of Bristol) are gratefully acknowledged. We thank the Leverhulme Trust for an Early Career Research Fellowship (S.J.G.) and the Royal Society and the Wolfson Foundation for a Research Merit Award (A.J.O.E).

References

1 R. D. Levine, *Molecular Reaction Dynamics*. (Cambridge University Press, Cambridge, 2005).

2 *Tutorials in Molecular Reaction Dynamics*, edited by M. Brouard and C. Vallance (Royal Society of Chemistry, Cambridge, 2010).

3 S. J. Greaves, R. A. Rose, and A. J. Orr-Ewing, Phys. Chem. Chem. Phys. **12** (32), 9129 (2010).

4 J. C. Owrutsky, D. Raftery, and R. M. Hochstrasser, Ann. Rev. Phys. Chem. **45**, 519 (1994).

5 G. A. Voth and R. M. Hochstrasser, J. Phys. Chem. **100**, 13034 (1996).

6 C. G. Elles and F. F. Crim, Ann. Rev. Phys. Chem. **57**, 273 (2006).

7 D. Raftery, M. Iannone, C. M. Phillips, and R. M. Hochstrasser, Chem. Phys. Lett. **201** (5-6), 513 (1993).

8 D. Raftery, E. Gooding, A. Romanovsky, and R. M. Hochstrasser, J. Chem. Phys. **101** (10), 8572 (1994).

9 L. Sheps, A. C. Crowther, C. G. Elles, and F. F. Crim, J. Phys. Chem. A **109** (19), 4296 (2005).

10 L. Sheps, A. C. Crowther, S. L. Carrier, and F. F. Crim, J. Phys. Chem. A **110** (9), 3087 (2006).

11 A. C. Crowther, S. L. Carrier, T. J. Preston, and F. F. Crim, J. Phys. Chem. A **112** (47), 12081 (2008).

12 A. C. Crowther, S. L. Carrier, T. J. Preston, and F. F. Crim, J. Phys. Chem. A **113** (16), 3758 (2009).

13 S. L. Carrier, T. J. Preston, M. Dutta, A. C. Crowther, and F. F. Crim, J. Phys. Chem. A **114** (3), 1548 (2010).

14 S. J. Greaves, R. A. Rose, T. A. A. Oliver, D. R. Glowacki, M. N. R. Ashfold, J. N. Harvey, I. P. Clark, G. M. Greetham, A. W. Parker, M. Towrie, and A. J. Orr-Ewing, Science **331**, 1423 (2011).

15 A. M. Smith, S. L. Coy, W. Klemperer, and K. K. Lehmann, J. Mol. Spectrosc. **134** (1), 134 (1989).

[16] A. E. Douglas and D. Sharma, J. Chem. Phys. **21** (3), 448 (1953).
[17] G. A. Bethardy, F. J. Northrup, and R. G. Macdonald, J. Chem. Phys. **105** (11), 4533 (1996).
[18] G. A. Bethardy, F. J. Northrup, and R. G. Macdonald, J. Chem. Phys. **102** (20), 7966 (1995).
[19] L. R. Copeland, F. Mohammad, M. Zahedi, D. H. Volman, and W. M. Jackson, J. Chem. Phys. **96** (8), 5817 (1992).
[20] C. Huang, W. Li, A. D. Estillore, and A. G. Suits, J. Chem. Phys. **129** (7), 074301 (2008).
[21] E. Arunan, G. Manke, and D. W. Setser, Chem. Phys. Lett. **207** (1), 81 (1993).
[22] V. R. Morris, F. Mohammad, L. Valdry, and W. M. Jackson, Chem. Phys. Lett. **220** (6), 448 (1994).
[23] E. Arunan and D. W. Setser, J. Phys. Chem. **95** (11), 4190 (1991).
[24] G. M. Greetham, P. Burgos, Q. Cao, I. P. Clark, P. S. Codd, R. C. Farrow, M. W. George, M. Kogimitzis, P. Matousek, A. W. Parker, M. R. Pollard, D. A. Robinson, Z. J. Xin, and M. Towrie, Appl. Spectrosc. **64**, 1311 (2010).
[25] A. C. Moskun and S. E. Bradforth, J. Chem. Phys. **119** (8), 4500 (2003).
[26] A. C. Moskun, A. E. Jailaubekov, S. E. Bradforth, G. H. Tao, and R. M. Stratt, Science **311** (5769), 1907 (2006).
[27] G. A. Bethardy, F. J. Northrup, G. He, I. Tokue, and R. G. Macdonald, J. Chem. Phys. **109** (11), 4224 (1998).
[28] I. Benjamin, J. Chem. Phys. **103**, 2459 (1995).
[29] D. R. Glowacki, R. A. Rose, S. J. Greaves, A. J. Orr-Ewing, and J. N. Harvey, submitted (2011).
[30] P. Botschwina, Chem. Phys. **81** (1-2), 73 (1983).
[31] V. Samant and J. F. Hershberger, Chem. Phys. Lett. **460**, 64 (2008).
[32] *NIST Chemistry Webbook, NIST Standard Reference Database Number 69*, edited by P. J. Linstrom and W. G. Mallard (Gaithersburg MD, 20899).
[33] J. Larsen, D. Madsen, J. A. Poulsen, T. D. Poulsen, S. R. Keiding, and J. Thogersen, J. Chem. Phys. **116** (18), 7997 (2002).
[34] J. Helbing, M. Chergui, S. Fernandez-Alberti, J. Echave, N. Halberstadt, and J. A. Beswick, Phys. Chem. Chem. Phys. **2**, 4131 (2000).
[35] U. Samuni, S. Kahana, R. Fraenkel, Y. Haas, D. Danovich, and S. Shaik, Chem. Phys. Lett. **225** (4-6), 391 (1994).
[36] D. R. Glowacki, A. J. Orr-Ewing, and J. N. Harvey, J. Chem. Phys. (submitted) (2011).